Organic & Biomolecular Chemistry

ROYAL SOCIETY OF CHEMISTRY

COMMUNICATION

View Article Online
View Journal | View Issue

Cite this: *Org. Biomol. Chem.*, 2020, **18**, 6509

Received 30th July 2020,
Accepted 10th August 2020

DOI: 10.1039/d0ob01577f

rsc.li/obc

Synthesis of functional 1,2-dithiolanes from 1,3-bis-*tert*-butyl thioethers†

Georg M. Scheutz,[a] Jonathan L. Rowell,[a] Fu-Sheng Wang,[b] Khalil A. Abboud,[a] Chi-How Peng [b] and Brent S. Sumerlin [a]*

We report the one-step synthesis of diversely substituted functional 1,2-dithiolanes by reacting readily accessible 1,3-bis-*tert*-butyl thioethers with bromine. The reaction proceeds to completion within minutes under mild conditions, presumably *via* a sulfonium-mediated ring closure. Using X-ray crystallography and UV-vis spectroscopy, we demonstrate how substituent size and ring substitution pattern can affect the geometry and photophysical properties of 1,2-dithiolanes.

1,2-Dithiolanes are five-membered heterocyclic molecules containing a disulfide bond. The intricate reactivity of this class of disulfides, arising from the geometric constraints imposed upon the sulfur–sulfur (S–S) bond, has been exploited for cell-uptake applications,[1–6] reversible protein–polymer conjugation,[7] biosensors,[8] dynamic networks,[9–14] and functional polymer synthesis.[15,16]

Distinct from linear disulfides, which usually exhibit CSSC dihedral angles around 90°, the five-membered cyclic geometry of 1,2-dithiolanes forces the disulfide scaffold into conformations with CSSC dihedral angles often lower than 35° (Fig. 1A and S1A†).[17,18] At such low dihedral angles, the neighboring fully occupied non-bonding sulfur orbitals overlap,[19,20] causing a destabilizing four-electron interaction, also known as closed-shell repulsion (Fig. S1A†).[21] This stereoelectronic effect weakens the S–S bond, rendering 1,2-dithiolanes prone to rapid thiol-disulfide exchange[22,23] and ring-opening polymerization.[7,16,24] Such polydisulfides generated from 1,2-dithiolanes are typically dynamic and can be reversibly depolymerized,[12,25,26] a phenomenon that has been exploited for the direct polydisulfide-mediated cytosolic delivery of various cargo,[27] such as proteins,[5] quantum dots,[28] or silica particles.[29]

In addition to the CSSC dihedral angle, a determining factor for the reactivity of 1,2-dithiolanes is the ring substitution pattern.[12,30,31] For example, Matile's group reported profound differences in the polymerization behavior[24] and the cell-uptake efficiency[2] of lipoic acid and asparagusic acid (Fig. 1A). Whitesides and coworkers showed that higher-substituted 1,2-dithiolanes are more resistant towards reduction and ring-opening (Fig. S1B†).[22] Considering these results, we believe there is great potential in controlling 1,2-dithiolane reactivity *via* tailored substituent selection. However, most application-focused reports revolve around commercially avail-

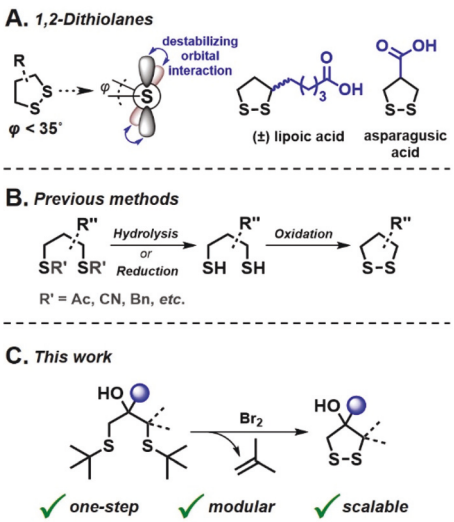

Fig. 1 Electronic properties and synthesis of 1,2-dithiolanes. (A) The low CSSC dihedral angle (φ) imparts 1,2-dithiolanes, such as lipoic or asparagusic acid, with unique reactivity. (B) Previous syntheses of 1,2-dithiolanes involved a two-step reaction sequence. (C) Our strategy provides hydroxy-functional 1,2-dithiolanes in a single step from readily available 1,3-bis-*tert*-butyl thioether substrates.

[a]*George & Josephine Butler Polymer Research Laboratory, Center for Macromolecular Science & Engineering, Department of Chemistry, University of Florida, Gainesville, FL 32611, USA. E-mail: sumerlin@chem.ufl.edu*

[b]*Department of Chemistry and Frontier Research Center on Fundamental and Applied Sciences of Matters, National Tsing Hua University, 101, Sec 2, Kuang-Fu Rd., Hsinchu 30013, Taiwan*

†Electronic supplementary information (ESI) available: Procedures, calculations, and characterization data. CCDC 2011482 and 2011483. For ESI and crystallographic data in CIF or other electronic format see DOI: 10.1039/d0ob01577f

able lipoic acid (Fig. 1A) and its amide or ester derivatives. This lack of substrate variety is arguably due to the limited synthetic accessibility of substituted 1,2-dithiolane derivatives with functional handles for downstream modification. 1,2-Dithiolanes are commonly synthesized in a two-step sequence, which includes generation of the 1,3-dithiol *via* hydrolysis or reduction of suitable precursors, followed by oxidation to the corresponding 1,2-dithiolane (Fig. 1B). However, formation of the 1,3-dithiol often requires harsh reaction conditions that limit functional group tolerance and often lead to undesired polydisulfide formation. To overcome these synthetic limitations and expand the substrate toolbox for applications of 1,2-dithiolanes, we developed a modular one-step synthesis of diversely substituted 1,2-dithiolanes from readily accessible 1,3-bis-*tert*-butyl thioethers (Fig. 1C). Furthermore, the 1,3-bis-*tert*-butyl thioethers were designed to feature a hydroxy group that can be used as a handle for downstream functionalizations of the 1,2-dithiolane product.

tert-Butyl protection of thiols is typically known for robustness and stability.[32,33] However, Mayor[34] and later Feringa[35] leveraged the *tert*-butyl group for the direct transformation of *S-tert*-butyl thioethers into thioacetates using acetyl chloride and a catalytic amount of Br_2 or $TiCl_4$, respectively. Specifically intriguing to us was Mayor's observation of disulfide side products during the reaction.[34] Based on these reports, we tested if *S-tert*-butyl cleavage in combination with intramolecular disulfide formation promoted by electrophilic halogen reagents could provide access to 1,2-dithiolanes from 1,3-bis-*tert*-butyl thioethers in a single step. Optimization of the reaction conditions with thioether **1a** as a substrate showed that Br_2, in combination with hydrated silica gel, was most effective for the targeted transformation, yielding 4-hydroxy-4-phenyl-1,2-dithiolane **PhDL** in 77% isolated yield (Table 1). The addition of silica gel to the reaction mixture improved the yield (entries 1 and 2), presumably by scavenging reactive byproducts,[36] which could be visually confirmed by the discoloration of the silica gel over the course of the reaction. While the slow addition of 1.3 equivalents of Br_2 typically led to full conversion of **1a**, lower reaction temperatures required increased amounts of Br_2 for the reaction to complete (entry 3). Other electrophilic halogen reagents, such as *N*-bromosuccinimide (NBS) or 1,2-dibromotetrachloroethane ($C_2Cl_4Br_2$), were less effective or showed no reaction (entries 4–6).

Analysis of the crude reaction mixture by ^{1}H NMR spectroscopy and GC-MS showed the formation of 1,2-dibromo-2-methylpropane and *tert*-butyl bromide as the major byproducts (Fig. S2–5†). Based on these results, we propose that ring closure proceeds *via* the initial formation of sulfonium bromide **A**,[37] followed by elimination of isobutylene (Fig. 2). The activated sulfenyl bromide **B** could then undergo intramolecular cyclization to compound **C**, which yields the target 1,2-dithiolane after another elimination of isobutylene. Isobutylene (T_b = −6.9 °C) either evaporates from the reaction mixture or reacts with Br_2 and HBr to form 1,2-dibromo-2-methylpropane and *tert*-butyl bromide, respectively (Fig. 2). The higher solubility of isobutylene in the mixture at lower temperatures would also explain the increased consumption of Br_2 at 0 °C (Table 1, entry 3).

Having established this synthetic strategy, we aimed to generate multiple 1,3-bis-*tert*-butyl thioether compounds (Fig. S6†) for the subsequent transformation into 1,2-dithiolanes (Fig. 1C). Specifically, we synthesized 1,3-bis-*tert*-butyl thioethers **1a–1l** from various 1,3-dichloropropan-2-ol derivatives, α,α′-halogenated ketones, and 2-(chloromethyl)oxiranes with *tert*-butylthiol and K_2CO_3 as a base in DMF at room temperature (Fig. S6†). This broad range of suitable starting materials suggests that a variety of 1,3-bis-*tert*-butyl thioether substrates can be readily generated by this protocol. Notably, the reaction could be conducted on multigram scales (**1a** and **1f**) and all products were obtained in good yield and purity, often without the need of chromatographic purification.

Following the 1,3-bis-*tert*-butyl thioether preparation, we used the optimized Br_2-induced ring-closure conditions (Table 1) to convert 1,3-bis-*tert*-butyl thioethers **1a–1f** and **1l** into 4-hydroxy-1,2-dithiolanes with moderate to good yields (Fig. 3). This approach provided access to seven new 1,2-dithiolane derivatives with unprecedented ring substitution and

Table 1 Optimization of reaction conditions[a]

Entry	Deviation from standard conditions	Yield [b] (%)
1	None	77
2	No silica gel	52
3[c]	0 °C	24
4[d]	NBS instead of Br_2	28
5	$C_2Cl_4Br_2$ instead of Br_2	n. r.
6	I_2 instead of Br_2	n. r.

[a] All reactions were run to full conversion of **1a** unless no reaction (n. r.) was observed. Standard conditions: **1a** (1.0 mmol), silica gel ([g silica gel]/[mmol **1a**] = 2), DCM (20 mL), room temperature (r. t.). [b] Isolated yield after column chromatography. [c] 2.2 equiv. Br_2. [d] 3 equiv. NBS.

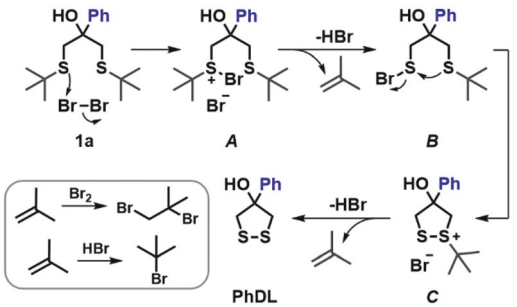

Fig. 2 Proposed reaction mechanism for the deprotection-disulfide formation sequence affording 4-hydroxy-4-phenyl-1,2-dithiolane (**PhDL**). After elimination, isobutylene either evaporates or is converted into brominated byproducts.

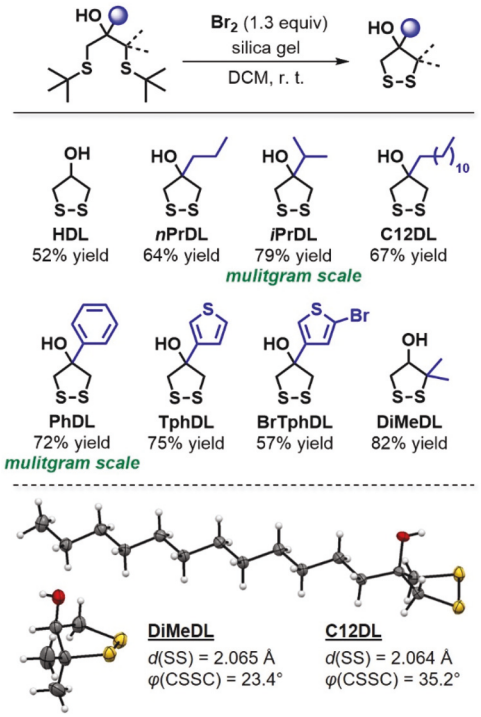

Fig. 3 Preparation of hydroxy-functional 1,2-dithiolanes with isolated yields. The lower yield of **HDL** is likely due to auto-polymerization during purification. The X-ray crystal structures of **DiMeDL** and **C12DL** show a shortened S–S bond length (*d*) and a compressed CSSC dihedral angle (φ).

functionality (Fig. 3). Geminal to the hydroxy group, the substituents were varied from hydrogen (**HDL**) to propyl (***n*PrDL**), isopropyl (***i*PrDL**), and dodecyl (**C12DL**); phenyl (**PhDL**), thiophenyl (**TphDL**), and bromothiophenyl (**BrTphDL**) groups could be installed as aromatic analogues. Additionally, we created an intriguing alternative 1,2-dithiolane scaffold with *gem*-dimethyl substitution vicinal to the disulfide bond (**DiMeDL**). Importantly, this reaction proved efficient on multigram scales (***i*PrDL** and **PhDL**), which will be beneficial in 1,2-dithiolane applications.

With the compounds in hand, we sought to evaluate the effect of substituent size and substitution pattern on 1,2-dithiolane ring conformation, since the geometry and dihedral angle of the disulfide moiety profoundly affects the properties of 1,2-dithiolanes (Fig. S1A†). The crystal structures of **C12DL** and **DiMeDL** (Fig. 3) revealed similarly elongated S–S bond lengths around 2.06 Å (linear disulfide bond lengths are typically around 2.03 Å)[17] but differing CSSC dihedral angles of 35.2° and 23.4°, respectively. Interestingly, this CSSC dihedral angle reduction coincided with a sharp decrease of the CCSS dihedral angle from 21° to 1° (Table S1†). Comparison with all available crystal structures of unbridged and monocyclic 1,2-dithiolanes showed a similar, almost linear relationship between the CSSC and the CCSS dihedral angles (Tables S1 and S2, Fig. S7†). We believe that such eclipsed CCSS conformations in 1,2-dithiolanes with low CSSC dihedral angles could potentially contribute to the reactivity associated with such compounds, warranting future investigations.

Next, we turned to UV-vis spectroscopy to analyze the maximum absorbance wavelength (λ_{max}) of the first electronic transition ($S_0 \rightarrow S_1$), which provides information about the S–S bond geometry in 1,2-dithiolanes. Specifically, the energy of $S_0 \rightarrow S_1$ in disulfides is dependent on the overlap of the fully occupied non-bonding sulfur orbitals, which in turn is determined by the CSSC dihedral angle (Fig. S1A†).[19,20] For example, a stronger orbital overlap at lower CSSC dihedral angles raises the HOMO energy while the LUMO remains largely unaffected,[20] thus reducing the photon energy required for the excitation of $S_0 \rightarrow S_1$.

For the 1,2-dithiolane products tested in this report, we recorded a slight increase of λ_{max} upon geminal substitution on C4 (Fig. 4, S8, and Table S3†). **HDL** exhibited a λ_{max} of 327 nm, whereas derivatives with alkyl and aromatic substituents on C4 showed λ_{max} values around 335 and 339 nm, respectively. The absorbance bands of derivatives with aromatic substituents were generally broader than those of derivatives with alkyl substituents, suggesting differences in the antibonding character of S_1.[38] Substitution on C3 in **DiMeDL** resulted in a large λ_{max} red shift to 354 nm, which corroborates with the lower CSSC dihedral angle revealed in the crystal structure. These results suggest that ring substitution affects the geometry and the photophysical properties of 1,2-dithio-

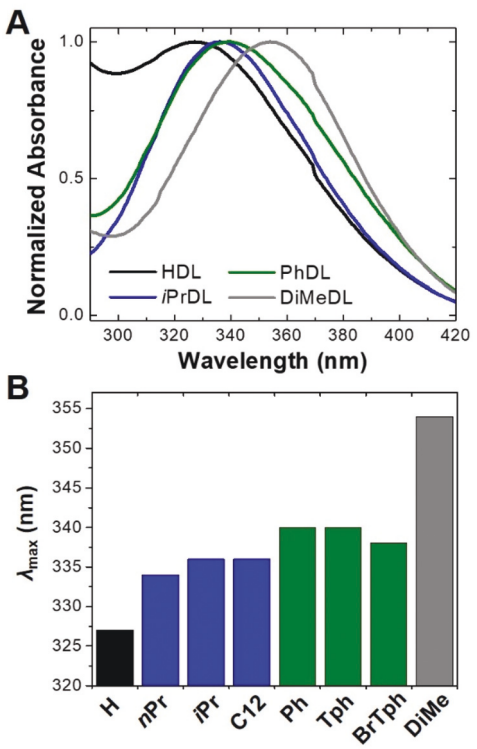

Fig. 4 Substituent effects on the photophysical properties of 1,2-dithiolanes. (A) Overlay of representative UV-vis absorbance spectra taken at 10 mM in DMSO. (B) Bar diagram showing the variation of the maximum absorbance wavelength (λ_{max}) with respect to 4-hydroxy-1,2-dithiolane substituent.

lanes. Furthermore, based on the linear increase of λ_{max} with C4 substituent A-values (Fig. S9†), we propose that the substituent effects in this position are mostly of steric nature.

Typically, low CSSC dihedral angles in 1,2-dithiolane compounds are associated with ring strain and S–S bond instability. For example, auto-polymerization has been commonly observed for 1,2-dithiolanes,[12,18,25,39,40] an issue we also encountered during purification of the compounds. We noted dramatic stability differences between **HDL** and higher substituted ***i*PrDL**, and **C12DL**. For example, **HDL** could be used only in solution due to rapid polymerization upon concentration, whereas ***i*PrDL** and **C12DL** were bench-stable over weeks. While the crystalline nature of **C12DL** could have a stabilizing effect, **HDL** and ***i*PrDL** are liquids and still showed substantial differences in stability.

To further investigate this observation, we estimated the ring strain for **HDL** and ***i*PrDL** *via* quantum chemical calculations of the enthalpy of reaction ($\Delta_{rxn}H$) for the isodesmic reaction between 1,4-butanedithiol (**BuSH**) and **HDL** or ***i*PrDL** (Table 2). The value of $\Delta_{rxn}H$ reflects the additional ring strain of the 1,2-dithiolane compound with respect to the relatively unstrained 1,2-dithiane (**BuSS**). The calculations revealed a $\Delta_{rxn}H$ of −27.9 kJ mol^{-1} for **HDL**, which is slightly higher than the ring strain for 1,2-dithiolane determined by Sunner[41] *via* iodine oxidation. Upon geminal substitution on C3 with an isopropyl group, $\Delta_{rxn}H$ was reduced to −2.9 kJ mol^{-1}, corroborating with the higher stability of ***i*PrDL** observed experimentally, emphasizing the stabilizing effect from substitution in cyclic structures.[12,22,42,43]

Finally, to test if the hydroxy group incorporated in the 1,2-dithiolane structure was suitable for downstream modifications, we reacted **PhDL** with isobutyryl chloride, affording 1,2-ditholane ester **2** in good yield (Fig. 5). Using the same strategy, we synthesized 1,2-dithiolane acrylate **3** from ***i*PrDL** and acryloyl chloride. The subsequent base-catalyzed thia-Michael addition between benzyl mercaptan and **3** provided Michael adduct **4** in high yield. We believe that such transformations could be particularly useful in applications that require covalent conjugation of 1,2-dithiolanes to substrates such as proteins or polymers.

Table 2 Ring strain calculations *via* the isodesmic reaction of 1,4-butanedithiol (**BuSH**) and 1,2-dithiane (**BuSS**) with a 1,2-dithiolane derivative in the ring-closed (**DL**) and 1,3-dithiol (**C3SH**) form

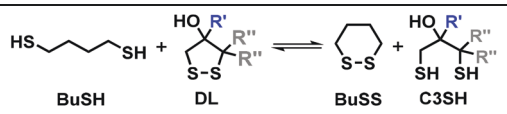

R′	R″	Compound	$\Delta_{rxn}H$ [a] (kJ mol^{-1})	λ_{max} [b] (nm)
H	H	**HDL**	−27.9	327
*i*Pr	H	***i*PrDL**	−2.9	336

[a] Calculated *via* $\Delta_{rxn}H$ = [Δ_fH (**BuSS**) + Δ_fH (**C3SH**)] − [Δ_fH (**BuSH**) + Δ_fH (**DL**)] All enthalpies of formation (Δ_fH) were calculated for the gas phase at 298 K using a B3LYP/6-311G** basis set. [b] Determined from UV-vis spectroscopy (Table S4†). Higher λ_{max} values indicate lower CSSC dihedral angles.

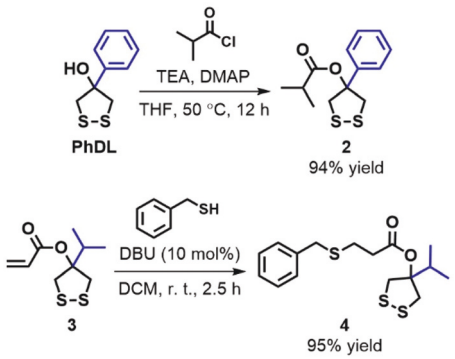

Fig. 5 Downstream functionalization of 1,2-dithiolanes, exploiting the hydroxy functionality. Triethylamine (TEA) was used as a base with 4-dimethylaminopyridine (DMAP) as a catalyst in the esterification of **PhDL**. 1,8-Diazabicylcoundec-7-ene (DBU) was employed in the base-catalyzed thia-Michael addition of 1,2-dithiolane acrylate **3** with benzyl mercaptan.

In conclusion, we disclosed a scalable and straightforward synthetic protocol for diversely substituted new 1,2-dithiolane compounds featuring a hydroxy functionality as a valuable handle for downstream conjugation. X-ray crystallography, UV-vis spectroscopy, and quantum chemical calculations revealed profound substitution effects on the stereoelectronic properties and the stability of the 1,2-dithiolane derivatives, suggesting that 1,2-dithiolane reactivity can be tuned by careful substituent selection. We believe this report represents an attractive avenue for the future design of 1,2-dithiolanes in advanced applications, such as cargo delivery and stimuli-responsive polymer materials.

Conflicts of interest

The authors have no conflicts to declare.

Acknowledgements

This research was supported by the DoD (W911NF-17-1-0326) and the NSF (DMR-1904631, CHE-1808234). The University of Florida Department of Chemistry Mass Spectrometry Center acknowledges NIH (S10 OD021758-01A1), and K.A.A wishes to acknowledge NSF for funding the X-ray diffractometer through CHE-1828064. The authors thank Prof. Yuan-Chung Cheng (National Taiwan University) for providing the calculation resource and Dr. Ion Ghiviriga (University of Florida) for assistance with NOE experiments.

Notes and references

1 G. Gasparini, E. K. Bang, G. Molinard, D. V. Tulumello, S. Ward, S. O. Kelley, A. Roux, N. Sakai and S. Matile, *J. Am. Chem. Soc.*, 2014, **136**, 6069–6074.

2 G. Gasparini, G. Sargsyan, E. K. Bang, N. Sakai and S. Matile, *Angew. Chem., Int. Ed.*, 2015, **54**, 7328–7331.
3 D. Abegg, G. Gasparini, D. G. Hoch, A. Shuster, E. Bartolami, S. Matile and A. Adibekian, *J. Am. Chem. Soc.*, 2017, **139**, 231–238.
4 J. Fu, C. Yu, L. Li and S. Q. Yao, *J. Am. Chem. Soc.*, 2015, **137**, 12153–12160.
5 L. Qian, J. Fu, P. Yuan, S. Du, W. Huang, L. Li and S. Q. Yao, *Angew. Chem., Int. Ed.*, 2018, **57**, 1532–1536.
6 N. Chuard, G. Gasparini, D. Moreau, S. Lorcher, C. Palivan, W. Meier, N. Sakai and S. Matile, *Angew. Chem., Int. Ed.*, 2017, **56**, 2947–2950.
7 J. Lu, H. Wang, Z. Tian, Y. Hou and H. Lu, *J. Am. Chem. Soc.*, 2020, **142**, 1217–1221.
8 L. Zhang, D. Duan, Y. Liu, C. Ge, X. Cui, J. Sun and J. Fang, *J. Am. Chem. Soc.*, 2014, **136**, 226–233.
9 Q. Zhang, C.-Y. Shi, D.-H. Qu, Y.-T. Long, B. L. Feringa and H. Tian, *Sci. Adv.*, 2018, **4**, eaat8192.
10 Q. Zhang, Y.-X. Deng, H.-X. Luo, C.-Y. Shi, G. M. Geise, B. L. Feringa, H. Tian and D.-H. Qu, *J. Am. Chem. Soc.*, 2019, **141**, 12804–12814.
11 G. A. Barcan, X. Zhang and R. M. Waymouth, *J. Am. Chem. Soc.*, 2015, **137**, 5650–5653.
12 X. Zhang and R. M. Waymouth, *J. Am. Chem. Soc.*, 2017, **139**, 3822–3833.
13 Y. Deng, Q. Zhang, B. L. Feringa, H. Tian and D.-H. Qu, *Angew. Chem., Int. Ed.*, 2020, **59**, 5278–5283.
14 G. M. Scheutz, J. L. Rowell, S. T. Ellison, J. B. Garrison, T. E. Angelini and B. S. Sumerlin, *Macromolecules*, 2020, **53**, 4038–4046.
15 H. Tang and N. V. Tsarevsky, *Polym. Chem.*, 2015, **6**, 6936–6945.
16 Y. Liu, Y. Jia, Q. Wu and J. S. Moore, *J. Am. Chem. Soc.*, 2019, **141**, 17075–17080.
17 R. Steudel, *Angew. Chem., Int. Ed. Engl.*, 1975, **14**, 655–664.
18 L. Teuber, *Sulfur Rep.*, 1990, **9**, 257–333.
19 G. Bergson, *Ark. Kemi*, 1958, **12**, 233–237.
20 D. B. Boyd, *J. Am. Chem. Soc.*, 1972, **94**, 8799–8804.
21 E. V. Anslyn and D. A. Dougherty, *Modern Physical Organic Chemistry*, University Science Books, Sausalito, California, 2006.
22 J. Houk and G. M. Whitesides, *J. Am. Chem. Soc.*, 1987, **109**, 6825–6835.
23 R. W. Singh and G. M. Whitesides, *J. Am. Chem. Soc.*, 1990, **112**, 6304–6309.
24 E. K. Bang, G. Gasparini, G. Molinard, A. Roux, N. Sakai and S. Matile, *J. Am. Chem. Soc.*, 2013, **135**, 2088–2091.
25 B. Nelander, *Acta Chem. Scand.*, 1971, **25**, 1510–1511.
26 J. P. Danehy and V. J. Elia, *J. Org. Chem.*, 1972, **37**, 369–373.
27 S. Du, S. S. Liew, L. Li and S. Q. Yao, *J. Am. Chem. Soc.*, 2018, **140**, 15986–15996.
28 E. Derivery, E. Bartolami, S. Matile and M. Gonzalez-Gaitan, *J. Am. Chem. Soc.*, 2017, **139**, 10172–10175.
29 C. Yu, L. Qian, J. Ge, J. Fu, P. Yuan, S. C. Yao and S. Q. Yao, *Angew. Chem., Int. Ed.*, 2016, **55**, 9272–9276.
30 A. Carmine, Y. Domoto, N. Sakai and S. Matile, *Chem. Eur. J.*, 2013, **19**, 11558–11563.
31 J. A. Burns and G. M. Whitesides, *J. Am. Chem. Soc.*, 1990, **112**, 6296–6303.
32 P. G. M. Wuts, *Greene's Protective Groups in Organic Synthesis*, John Wiley & Sons, New Jersey, 2014.
33 O. Nishimura, C. Kitada and M. Fujino, *Chem. Pharm. Bull.*, 1978, **26**, 1576–1585.
34 A. Błaszczyk, M. Elbing and M. Mayor, *Org. Biomol. Chem.*, 2004, **2**, 2722–2724.
35 T. C. Pijper, J. Robertus, W. R. Browne and B. L. Feringa, *Org. Biomol. Chem.*, 2015, **13**, 265–268.
36 M. H. Ali and M. McDermott, *Tetrahedron Lett.*, 2002, **43**, 6271–6273.
37 E. Anklam, *Synthesis*, 1987, 841–843.
38 L. Antonov and D. Nedeltcheva, *Chem. Soc. Rev.*, 2000, **29**, 217–227.
39 G. Claeson, *Acta Chem. Scand.*, 1955, **9**, 178–180.
40 L. Field and R. B. Barbee, *J. Org. Chem.*, 1969, **34**, 36–41.
41 S. Sunner, *Nature*, 1955, **176**, 217.
42 M. E. Jung and G. Piizzi, *Chem. Rev.*, 2005, **105**, 1735–1766.
43 H. Liu, A. Z. Nelson, Y. Ren, K. Yang, R. H. Ewoldt and J. S. Moore, *ACS Macro Lett.*, 2018, **7**, 933–937.